

Electrical properties of transition-metal carbides of group IV

F. A. Modine, M. D. Foegelle,* C. B. Finch, and C. Y. Allison[†]

Solid State Division, Oak Ridge National Laboratory, Oak Ridge, Tennessee 37831-6030

(Received 15 May 1989)

Electrical resistivities of six single crystals of group-IVB transition-metal carbides are reported for temperatures between 4 and 1000 K. Hall coefficients of the crystals are reported for temperatures to 350 K. The chemical analyses of the ratio of carbon-to-metal atoms in the crystals (0.89 to 0.99) were verified by an inverse linear relationship between the carbon-vacancy concentration and the low-temperature Hall mobilities. Bloch-Grüneisen theory provides a fit to the temperature dependence of the resistivity data that passes the χ^2 test for TiC_x and ZrC_x but not for $\text{HfC}_{0.99}$. The measurements reveal a tendency toward resistivity saturation at high temperature that is well described by a parallel-resistance model in which the saturation resistivity corresponds to a carrier mean free path roughly equal to the lattice constant. The measurements are compared to earlier experimental studies and to predictions of band-structure calculations. Theories of electronic transport are evaluated.

I. INTRODUCTION

Few systematic studies have been made of the electrical properties of transition-metal-carbide single crystals over a wide temperature range. Hence, there is little basis for theoretical interpretations of the electronic transport. Numerous studies of electrical properties of transition-metal carbides have been reported.¹⁻¹¹ However, most of these studies have yielded incomplete or uncertain results for the following reasons: (1) the measurements were often restricted to near ambient temperature; (2) polycrystalline samples, which require uncertain corrections for their porosity, were usually measured; and (3) the composition of the samples was often not well characterized. This last consideration is especially important, since the carbon sublattice of these materials can accommodate nearly 50% vacancies and retain the rocksalt cubic structure. Such large numbers of vacancies strongly influence the electrical properties and make accurate knowledge of the composition essential.

We previously published a systematic study of the temperature dependence of the electrical resistivities of four single-crystal transition-metal carbides.¹ The study revealed resistivities that are well described by either the Bloch-Grüneisen or the Wilson equations for electron transport in metals, depending upon whether or not the crystals exhibit superconductivity above liquid-helium temperature. The study is extended in this paper to include five additional crystals. Also, the resistivity measurements are extended in temperature from 350 to 1000 K. These data allow an interpretation of resistivity saturation at high temperatures for the transition-metal carbides. In addition, Hall coefficients are reported for temperatures between 4 and 350 K. The measurements provide information about the change of carrier density with composition and indicate that the low-temperature Hall mobility is inversely proportional to the carbon-vacancy concentration, independent of the metal constituent. Hence, electrical-properties data per se verify the carbon

content of the crystals and thereby ensure the quality of the results in this important aspect. Moreover, the measurements enable critical comparisons with other experimental results, with results of band-structure calculations, and with transport theory.

II. EXPERIMENTAL ASPECTS

Transition-metal carbide single crystals were grown by the rf floating-zone method, with the exception of an HfC crystal which was prepared by a strain-anneal method. Crystals of $\text{TiC}_{0.95}$, $\text{ZrC}_{0.98}$, and $\text{ZrC}_{0.93}$ were grown at Oak Ridge National Laboratory (ORNL) and chemically analyzed by Teledyne Wah Chang of Albany, Oregon, to establish carbon content. Crystals of $\text{TiC}_{0.92}$ and $\text{ZrC}_{0.89}$ were grown at Martin Marietta Laboratories by W. Precht, who provided the crystals and their compositions. The crystal of $\text{HfC}_{0.99}$, grown by Westinghouse Astronuclear Laboratory, was obtained from H. G. Smith of ORNL, who purchased it from Alpha Crystals. This crystal exhibited a grain boundary and a small pore and was of poorer quality than the other samples. All crystals were cut into platelets with a thickness of about 0.5 mm and lateral dimensions of several millimeters.

Electrical resistivities and Hall coefficients were measured by the method of van der Pauw¹² using currents of 0.3–1.0 A. The measurement sequence was automated using a scanner controlled by a computer, which also performed stability checks on the measurements, controlled the temperature, acquired the data, and analyzed the results. Measurements between 4 and 350 K employed a liquid-transfer refrigeration system. Rhodium-plated, spring-loaded contacts made electrical connection to the sample, which was insulated from a copper cold finger by a thin sapphire plate. Temperature was controlled and measured using GaAs thermometers mounted on the cold finger. At temperatures between 300 and 1000 K, a clam shell furnace was used. A crystal was held by a jig made of macor and alumina in an evacuated quartz tube. Plati-

num electrical contacts to the sample were spring-loaded from outside the hot zone of the furnace. Temperature was sensed by a NiCr/NiAl type-K thermocouple and controlled with a digital controller.

High- and low-temperature measurements were combined by adjusting one of the data sets with a multiplicative factor to obtain agreement in their region of overlap between 300 and 350 K. This adjustment was usually no more than 1%, and it can be attributed to minor differences in the contact placement. The absolute accuracy of the resistivity measurements is limited by uncertainty in sample and contact geometry and is estimated at 3%. Precision and relative accuracy are much better. Typical measurements exhibited a standard deviation of about 50 nΩ cm. However, the accuracy of temperature control is estimated at 1 K, which contributes an additional 50 nΩ cm of uncertainty to a typical resistivity measurement. Although temperature control is poorer near liquid-helium temperature, a much lower temperature coefficient of the resistivity tends to compensate. The total uncertainty contributed by the measurements combined with the temperature uncertainty is estimated to be 70 nΩ cm.

The absolute accuracy of the Hall measurements is also estimated at 3% because it results from the same geometrical factors. The standard deviation of the Hall measurements is typically about $2 \times 10^{-11} \text{ m}^3/\text{C}$, and the 1 K temperature uncertainty contributes about $1 \times 10^{-11} \text{ m}^3/\text{C}$, so the total statistical error is about $2.2 \times 10^{-11} \text{ m}^3/\text{C}$. However, five separate measurements were usually averaged to obtain a final error estimated at $1 \times 10^{-11} \text{ m}^3/\text{C}$.

III. RESULTS AND DISCUSSION

Resistivities and Hall coefficients measured at temperatures between 4 and 350 K are shown in Figs. 1 and 2 for the nearly stoichiometric crystals $\text{ZrC}_{0.98}$ and $\text{HfC}_{0.99}$. The least-squares method was used to fit theoretical expressions (shown as solid curves) to the resistivities. The

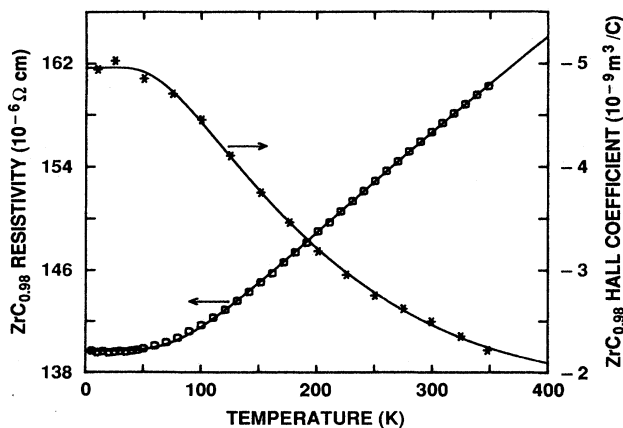


FIG. 1. The resistivity and Hall coefficient of $\text{ZrC}_{0.98}$ measured between 4 and 350 K. Bloch-Grüneisen theory has been fit to the resistivity data.

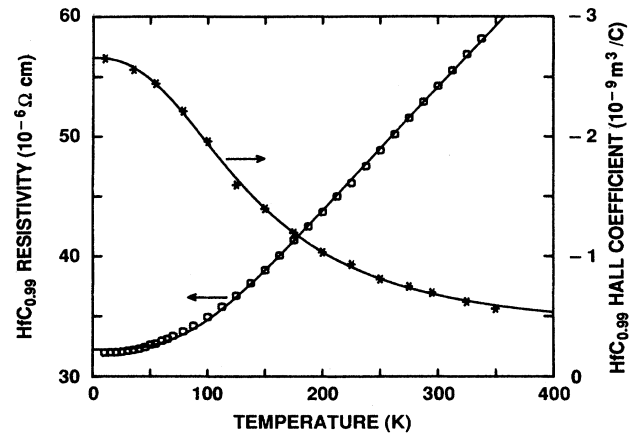


FIG. 2. The resistivity and Hall coefficient of $\text{HfC}_{0.99}$ measured between 4 and 350 K. Wilson theory has been fit to the resistivity data.

best fit to the $\text{ZrC}_{0.98}$ resistivity was obtained with the Bloch-Grüneisen expression:

$$\rho(T) = \rho_0 + 4\rho_1 T (T/\Theta)^4 J_5(\Theta/T). \quad (1)$$

The constant ρ_0 is the residual resistivity at low temperature, and ρ_1 is the derivative of the resistivity with respect to temperature in the high-temperature limit. The parameter Θ is a characteristic temperature which is equal to the Debye temperature in the Bloch-Grüneisen theory. The function $J_5(\Theta/T)$ is the transport integral defined by

$$J_n(\Theta/T) = 2^{n-1} \int_0^{\Theta/2T} x^n / \sinh^2 x \, dx, \quad (2)$$

where T is the absolute temperature. The best fit to the resistivity of the $\text{HfC}_{0.99}$ crystal is obtained with the Wilson expression:

$$\rho(T) = \rho_0 + 2\rho_1 T (T/\Theta)^2 J_3(\Theta/T). \quad (3)$$

As in Eq. (1), the expression is normalized so that ρ_1 is the slope of the resistivity curve at high temperature.

Table I gives parameter values that provide the best fits of Eqs. (1) or (3) to resistivity measurements at temperatures up to 350 K for all the crystals studied. The uncertainty of the parameter values and the standard deviation of the data about the curve were calculated by the method described by Bevington.¹³ The Bloch-Grüneisen equation gives the best fit to all resistivities except for the $\text{HfC}_{0.99}$ crystal. However, a relatively poor fit to the $\text{HfC}_{0.99}$ resistivity is obtained with either equation, and based upon our estimate of 70 nΩ cm for the variance of the resistivity measurements, neither fit of $\text{HfC}_{0.99}$ will pass the χ^2 test.

Several trends are apparent in Table I. The increase in residual resistivity ρ_0 with decreasing carbon content is logically attributed to electron scattering from carbon vacancies. The increase in ρ_1 with carbon content suggests that the carrier concentration decreases or that Matthiessen's rule is violated.³ Hall-data and band-structure calculations suggest that it is the carrier con-

TABLE I. Parameters describing the electrical resistivity of group-IVB transition-metal carbides at temperatures between 0 and 350 K. The values were obtained by fitting the data to the Bloch-Grüneisen expression, excepting that the second set of values for HfC was obtained from a fit to the Wilson model. Standard deviations of the parameters and of the data from the fitted function are given.

	ρ_0 ($\mu\Omega$ cm)	ρ_1 (n Ω cm/K)	Θ (K)	σ_ρ (n Ω cm)
TiC _{0.95}	145.5±0.0	44.01±0.13	718.6±5.6	55.5
TiC _{0.92}	165.5±0.0	39.11±0.16	737.2±5.1	45.4
ZrC _{0.98}	139.7±0.0	67.37±0.19	538.7±4.0	83.3
ZrC _{0.93}	180.8±0.0	48.98±0.15	569.7±4.6	64.9
ZrC _{0.89}	193.8±0.0	42.45±0.13	574.1±4.1	72.2
HfC _{0.99}	32.39±0.8	88.13±0.86	574.1±12.9	281.8
HfC _{0.99}	32.22±0.5	90.58±0.57	703.1±9.7	172.9

centration that decreases. The Θ values are in good agreement with Debye temperatures found from elastic-constant measurements, specific-heat measurements, and x-ray scattering.^{2,14} The Debye temperatures vary from about 400 to 900 K, with elastic constants giving the highest values and x-ray scattering giving the lowest values. In Table I, Θ varies from 539 to 703 K.

The resistivity data shown in Figs. 1 and 2 can be compared to similar measurements by Clinard and Kempter⁷ on hot-pressed, polycrystalline samples with a carbon content nearly identical to that of our single crystals. It is surprising that the residual resistivities of the polycrystalline samples are much lower than those of the single crystals. A polycrystalline sample of ZrC_{0.98} exhibited a ρ_0 of 26 $\mu\Omega$ cm, which is in striking contrast to the ρ_0 of 139.7 that we measured for a single crystal. Clinard and Kempter found residual resistivities of 17.3 and 13.5 $\mu\Omega$ cm for polycrystalline HfC_{0.98} and HfC_{0.97}, respectively, which is about a factor of 2 lower than we report for a single crystal of HfC_{0.99}. The explanation of these discrepancies is not clear, but in contrast to expectations, it is apparent that the polycrystalline samples have lower residual resistivities than do single crystals. Piper^{5,6} found that a single crystal of TiC_{0.96} has a resistivity much larger than that of the same material after being crushed and hot pressed. Clinard and Kempter⁷ also fitted the Bloch-Grüneisen expression to their resistivities, but they only used data for temperatures between 110 and 300 K for ZrC_{0.98} and between about 145 and 300 K for HfC_x. They found values for ρ_1 and Θ that are within about 20% of the values that we find for single crystals. This is good agreement considering the differences in the temperature ranges of the data that were fitted and the large differences in the values for ρ_0 .

Figure 3 shows Hall data measured at temperatures between 4 and 350 K for samples of TiC and ZrC that are well off stoichiometry. These data are well described by the empirical formula

$$R(T) = R_0 [1 - \exp(-T_0/T)], \quad (4)$$

where R_0 represents the low-temperature limit and T_0 is a characteristic temperature for the data. The solid curves of Fig. 3 represent least-squares fits of this formula to the data, and the parameters for the curves are given

in Table II. Unfortunately, Eq. (4) does not fit the more temperature-dependent data for the nearly stoichiometric crystals as well, and the Hall data of Figs. 1 and 2 have been fitted to smooth curves that have no simple mathematical expression. The magnitude, the dependence on carbon content, and the temperature variation of the Hall data are in reasonable agreement with measurements made by Williams⁴ and by Piper^{5,6} on single crystals of TiC_x. However, most of the Hall data of Table II are in poor agreement with measurements that have been made on polycrystalline samples.²

A crude interpretation of the Hall data can be made if a single band with a spherical Fermi surface is assumed, and the relaxation-time anisotropy is neglected. The Hall constant is then simply related to the carrier density N and the density of states at the Fermi surface $N(E_F)$:

$$R = A/eN \simeq (3m^3/\pi^4\hbar^6)/[N(E_F)]^3, \quad (5)$$

where A is an anisotropy factor, which is assumed equal to unity, although it is probably somewhat larger than unity. Values calculated for N and $N(E_F)$ using R_0 and a free-electron mass have been included in Table II. The values for $N(E_F)$ are less than half the 0.2–0.6 that is

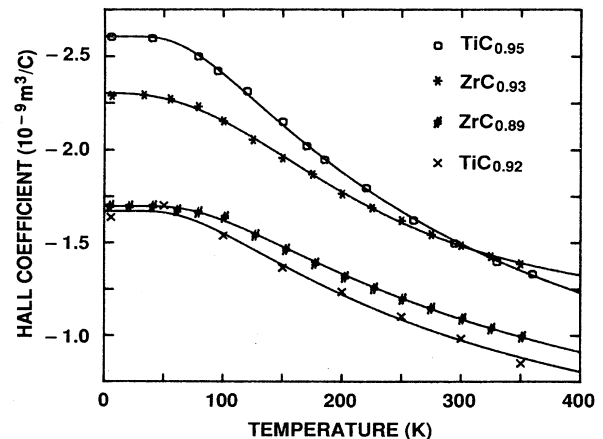


FIG. 3. Hall coefficients for samples of TiC_x and ZrC_x measured between 4 and 350 K.

TABLE II. Parameters describing the Hall coefficients of group-IVB transition-metal carbides. The low-temperature limit R_0 and the temperature T_0 are obtained from a fit of $R = R_0[1 - \exp(-T_0/T)]$ to the data. The electron density N and the density of states at the Fermi energy are obtained from R_0 by assuming a single carrier with an effective mass equal to the electron mass and a spherical Fermi surface. The E_p is a Drude-model plasma energy calculated from N .

	R_0 (mm ³ /C)	T_0 (K)	100N (1/cell)	$N(E_F)$ (1/eV cell)	E_p (eV)
TiC _{0.95}	-2.61	255	4.84	0.112	1.82
TiC _{0.92}	-1.67	262	7.58	0.129	2.27
ZrC _{0.98}	-4.96		3.27	0.115	1.32
ZrC _{0.93}	-2.27	312	7.13	0.150	1.95
ZrC _{0.89}	-1.70	307	9.14	0.165	2.24
HfC _{0.99}	-2.66		5.69	0.137	1.80

found from band-structure calculations for the materials.¹⁵⁻²² Somewhat better agreement with the calculations is obtained if room-temperature Hall data are used in Eq. (5). However, the agreement with band-structure calculations is good, considering the approximations made in Eq. (5). The temperature dependence of the data probably originates in the neglected anisotropy factor, although some investigators have attributed the temperature dependence to thermally generated carriers.^{3,4,9} Band-structure calculations also indicate an increase in $N(E_F)$ as the carbon content of the crystals decreases, which is a trend seen in the data of Table II. In fact, Marksteiner¹⁵ predicts a 54% increase in $N(E_F)$ for ZrC_x as x decreases from 0.98 to 0.89, which is in good agreement with the 43% increase seen in Table II. Other investigators computed carrier densities that are roughly twice those of Table II, primarily because they used room-temperature rather than low-temperature Hall data.²

Plasma frequencies can be computed from the carrier densities inferred from the Hall measurements. We write

$$E_p^2 = (\hbar\omega_p)^2 = (4\pi/3)(e^2\hbar^2)N(E_F)V_F^2 \approx 4\pi Ne^2/m, \quad (6)$$

where ω_p is the plasma frequency, E_p is the corresponding energy, and V_F is the Fermi velocity. Values for E_p of 1.3-2.2 eV are obtained from the densities of Table II and have been included in the table. The result for ZrC_{0.89} allows interesting comparisons. A value of $E_p = 2.2$ eV is obtained from the low-temperature Hall coefficient, but 3.4 eV is obtained from the room-temperature result. A previous study²³ of the room-temperature optical properties of this crystal yielded a value of 3.3 eV and a similar unpublished study of the TiC_{0.92} crystal yielded a value of 3.1 eV. Band-structure calculations²⁴ have yielded a value of 3.1 eV for a stoichiometric ZrC crystal. Room-temperature Hall coefficients appear to give a better prediction of the carrier concentrations than do low-temperature coefficients. However, this result is very likely fortuitous. The Hall measurements are more consistent with the optical results and the band-structure calculations if the anisotropy factor A is approximately 2 at low temperature and nearly unity at room temperature. The temperature dependence of A presumably results from the increasing impor-

ance of phonon scattering at high temperatures.

To the extent that the Hall coefficient measures the carrier density and the low-temperature resistivity is dominated by carbon-vacancy scattering, the Hall mobility at low temperature should be inversely proportional to the number of carbon vacancies. We write

$$\mu_0 = R_0/\rho_0 \approx eA/mV_F\sigma_V N_V, \quad (7)$$

where σ_V and N_V are the scattering cross section and the density, respectively, of carbon vacancies. Figure 4 is a plot of the inverse Hall mobility versus the vacancy concentration deduced from chemical analysis for all the crystals studied. The plot verifies Eq. (7), and it suggests that (1) the low-temperature Hall coefficient is inversely proportional to carrier density, (2) the low-temperature Hall mobility is independent of the metal constituent for the group-IVB transition-metal carbides, and (3) the carbon content of the crystals has been accurately determined. However, whereas a good fit to Eq. (7) implies

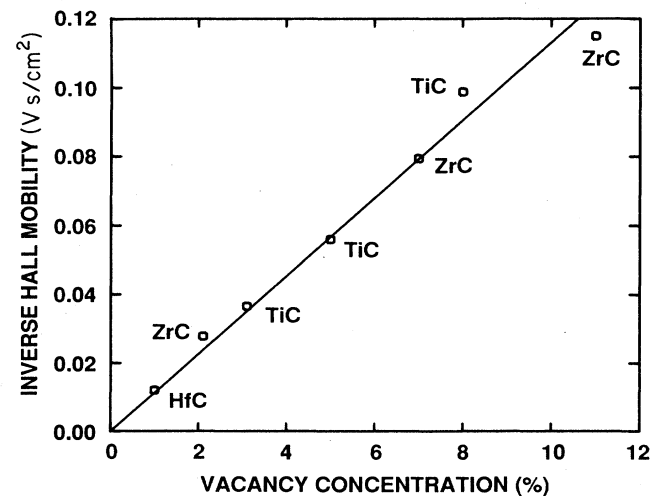


FIG. 4. Low-temperature inverse Hall mobilities of group-IV transition-metal carbides shown as a function of vacancy concentration. The result for TiC_{0.97} is from data of Williams (Ref. 4).

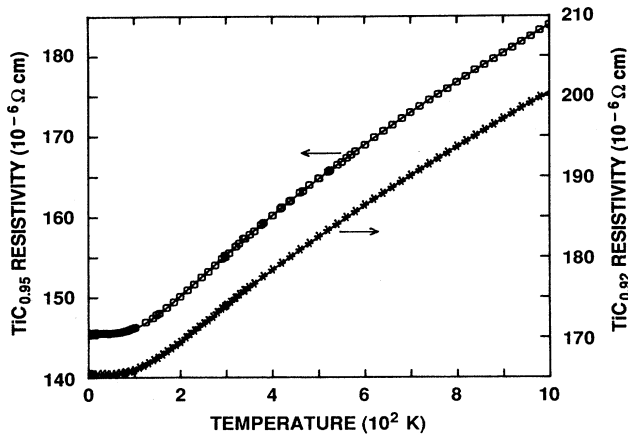


FIG. 5. The electrical resistivities of $\text{TiC}_{0.95}$ and $\text{TiC}_{0.92}$ measured between 4 and 1000 K.

that $A/\sigma_V V_F$ is material independent at low temperature, the Hall coefficient is inversely proportional to the carrier density only if A is individually material independent [see Eq. (5)]. A data point taken from results of Williams⁴ has been included in Fig. 4 to show consistency with an independent study by another researcher.

At high temperatures, the resistivities of transition-metal carbides deviate from the linear dependence on temperature predicted by the Bloch-Grüneisen and Wilson theories and tend to saturate at a constant value. Figures 5 and 6 show resistivity measurements at temperatures between 4 and 1000 K for crystals of TiC_x and ZrC_x . The data were fit with a parallel-resistance model in which the temperature-dependent resistivity is in parallel with a constant resistivity ρ_∞ .²⁵ We write

$$\rho(T) = \rho_{\text{id}}(T) / [1 + \rho_{\text{id}}(T) / \rho_\infty], \quad (8)$$

where the temperature-dependent contribution $\rho_{\text{id}}(T)$ is an idealized resistivity of either the Bloch-Grüneisen or the Wilson form [i.e., Eq. (1) or (3)]. Table III shows the parameters obtained by fitting Eq. (8) to the resistivities of the samples. The quality of the fits is similar to that described in Table I. The fits are excellent, but the fit to the $\text{HfC}_{0.99}$ data fails a χ^2 test for either the Bloch-Grüneisen or the Wilson temperature dependence.

In comparison to the values in Table I, the values of ρ_0 in Table III are increased by more than 50%, except for $\text{HfC}_{0.99}$. Hence, saturation effects are substantial even at the lowest temperatures for crystals with high residual resistivities. Moreover, the values for ρ_1 , which is a measure of the strength of the electron-phonon interaction, are increased by as much as a factor of 3 over the values in Table I. This implies that ρ_1 can be accurately determined only from measurements at temperatures that are high enough to allow ρ_∞ to be evaluated. A most surprising result is that the ρ_∞ values are more variable than the ρ_0 values and that ρ_∞ increases with the carrier density and defect concentration.

An increase in ρ_∞ with N is unexpected because the saturation resistivity is thought to be associated with a

decrease in the mean free path toward a minimum value equal to the interatomic spacing.^{26,27} We write

$$\begin{aligned} \rho_\infty &= m V_F / e^2 a N \simeq (\hbar / e^2) (3\pi^2 / a^3 N^2)^{1/3} \\ &\simeq 1.27 \times 10^{10} / a N^{2/3}, \end{aligned} \quad (9)$$

where a is the interatomic spacing and V_F is related to N using the spherical Fermi surface approximation. The right-hand expression yields ρ_∞ in $\mu\Omega \text{ cm}$ when a and N are measured in cm. Although the accuracy of the approximations is questionable, the predicted inverse relationship between ρ_∞ and N should be correct; but it is not observed in the results. Nevertheless, if the lattice constant is used for a and the optically determined plasma energy of 3.3 eV is used to calculate N for $\text{ZrC}_{0.89}$ from Eq. (6), a value for ρ_∞ of 681 $\mu\Omega \text{ cm}$ is found from Eq. (9). This is in rough agreement with the value of 574 $\mu\Omega \text{ cm}$ found from high-temperature resistivity measurements.

The temperature-dependent $\rho(T)$ is contributed by electron scattering from phonons which give a scattering cross section that is directly proportional to the temperature at evaluated temperature. The phonon contribution to the relaxation time at high temperature is

$$1/\tau_{e\text{-ph}} = \omega_p^2 \rho_1 T / 4\pi = 2\pi \lambda_{\text{tr}} k_B T / \hbar, \quad (10)$$

where λ_{tr} is the electron-phonon coupling parameter appropriate to electron transport, but which is approximately the mass enhancement λ that determines the superconducting transition temperature:^{28,29}

$$\lambda_{\text{tr}} = \rho_1 E_p^2 / 8\pi^2 \hbar k_B \simeq 0.248 \rho_1 E_p^2, \quad (11)$$

where the right-hand expression holds for ρ_1 in units of $\mu\Omega \text{ cm/K}$ and E_p in eV.

Values for λ_{tr} can be calculated from Eq. (11) by using parameters in Tables II and III. However, it is probably better to use optically determined values for E_p or to increase the E_p values in Table II by $\sqrt{2}$ to account for the anisotropy factor estimated as $A = 2$ at low temperature. Using the optical values of 3.1 and 3.3 eV for the plasma

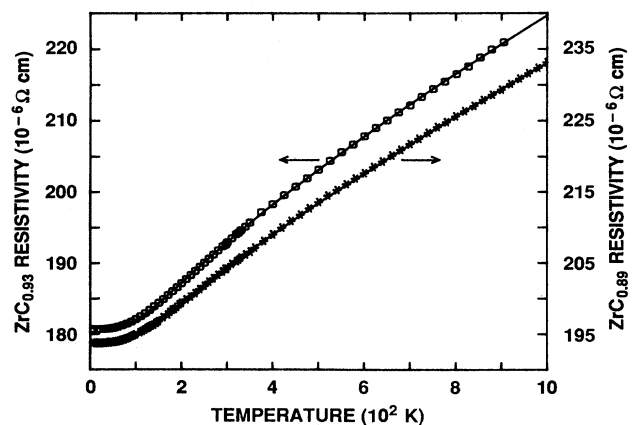


FIG. 6. The electrical resistivities of $\text{ZrC}_{0.93}$ and $\text{ZrC}_{0.89}$ measured between 4 and 1000 K.

TABLE III. Parameters describing the electrical resistivity of group-IVB transition-metal carbides at temperatures between 0 and 1000 K. The values were obtained by fitting the data to a parallel-resistor model in which the temperature-dependent resistivity is given by the Bloch-Grüneisen expression, excepting that the Wilson model of the temperature dependence was used for the second set of values for HfC. Standard deviations of the parameters and of the data from the fitted function are given.

	ρ_0 ($\mu\Omega$ cm)	ρ_1 (n Ω cm/K)	Θ (K)	ρ_∞ ($\mu\Omega$ cm)	σ_ρ (n Ω cm)
TiC _{0.95}	233.0±1.4	120.4±1.7	749.9±3.8	388.0±3.8	54.8
TiC _{0.92}	255.4±1.8	97.23±1.6	754.6±3.3	470.1±6.1	43.1
ZrC _{0.98}	238.9±0.6	226.3±1.6	720.1±3.3	343.5±1.7	62.7
ZrC _{0.93}	284.9±3.6	129.1±3.8	599.8±5.7	495.1±10.9	89.8
ZrC _{0.89}	296.7±3.2	105.3±2.6	609.9±4.6	559.0±11.4	81.9
HfC _{0.99}	34.11±0.10	104.5±1.0	619.4±7.7	675.3±26.2	236.2
HfC _{0.99}	34.06±0.07	107.7±0.7	742.8±6.3	608.2±13.8	148.6

energies of TiC_{0.92} and ZrC_{0.89} gives 0.23 and 0.28 for λ_{tr} , respectively. The ZrC_{0.98} crystal exhibits the highest value of ρ_1 in Table III, but the plasma energy is only 1.87 eV, even when adjusted for anisotropy, and $\lambda_{tr}=0.20$ is found from Eq. (11). The more nearly stoichiometric crystals exhibit higher temperature coefficients, but have lower carrier densities. Hence, it is unlikely that the electron-phonon-coupling parameter can exceed about 0.3 for group-IVB transition-metal carbides. Superconducting transition temperatures can be estimated by using the values found for Θ and λ_{tr} for Θ_D and λ , respectively, in the McMillian equation:³⁰

$$T_c = \frac{\Theta_D}{1.45} \exp \left[\frac{-1.04(1+\lambda)}{\lambda - \mu^*(1+0.62\lambda)} \right], \quad (12)$$

where μ^* is the Coulomb coupling constant which is usually estimated to be 0.10–0.13. The calculated transition temperatures are much less than 0.1 K, which is consistent with the absence of observable superconductivity in the group-IVB carbides.

Gurvitch recently proposed a universal phase diagram that associates λ and ρ_0 with n , the power-law exponent in the temperature dependence of the resistivity at low temperature.³¹ In his theory, the simultaneous presence of strong electron-phonon coupling (measured by λ) and disorder (measured by ρ_0) produces a transition from a classical region of $n = 3-5$ to a region of $n = 2$ at a phase boundary defined by

$$(\lambda - 0.7)\rho_0 = 13 \mu\Omega \text{ cm} . \quad (13)$$

The parameters for the group-IVB transition-metal carbides are consistent with this classification. At low temperature, the Bloch-Grüneisen and Wilson expressions vary as T^5 and T^3 , respectively, and the weak electron-phonon coupling (i.e., $\lambda < 0.7$) clearly places these materials in the classical region independent of their ρ_0 values.

IV. CONCLUSIONS

The Bloch-Grüneisen theory gives an excellent description of the temperature dependence of the electrical resistivities of the TiC_x and ZrC_x crystals, but a different temperature dependence is found for HfC_{0.99}. The Wilson model gives a better fit—but not a good fit—to the HfC_{0.99} data, whereas it gives an excellent fit to the resistivities of the superconducting transition-metal carbides of group VB.¹ Although the quality of the HfC_{0.99} crystal is suspect, it is probably not responsible for the different temperature dependence.

Although the Bloch-Grüneisen and Wilson models provide convenient descriptions of the resistivity data, there is no *a priori* reason to expect these descriptions to be accurate. Both models are based upon restrictive assumptions. The Bloch-Grüneisen equation is obtained from a lowest-order variational approximation to the Boltzmann equation in which a rigid shift of the Fermi surface and a Debye phonon spectrum are assumed, and the Wilson equation assumes electron scattering between *s* and *d* bands that is improbable in the transition-metal carbides.

There are significant differences between the resistivities (and also the Hall coefficients) of single-crystal and polycrystalline samples⁷ of the same transition-metal carbide. The lower residual resistivities of polycrystalline samples are especially remarkable because single crystals should have more nearly perfect order and, therefore, should exhibit less defect and grain-boundary scattering. The origin of these differences in electrical properties is unknown.

The Hall measurements are particularly valuable because they verify the carbon content of the crystals, which is too often a deficiency of other studies, and in so doing suggest that carrier densities can be inferred from the low-temperature Hall coefficients. Clearly, the carrier densities are uncertain to within a temperature-dependent anisotropy factor that decreases as the relative importance of phonon and defect scattering changes with temperature. Even larger uncertainties enter into the calculations of plasma frequencies and densities of states, because the Fermi velocity and effective mass should take Fermi surface geometry into accurate account. Nevertheless, the implied change in these parameters with carbon content roughly agrees with band-structure calculations.

The transition-metal carbides exhibit a tendency toward resistivity saturation at elevated temperature, which is well described by the parallel-resistance model. However, the results imply a saturation resistance that increases with the carbon-vacancy concentration. This is surprising because both the Hall measurements and band-structure calculations suggest that the carrier concentration increases with the carbon-vacancy concentration. Hence, the saturation resistance should decrease rather than increase. The reason for the increase is obscure, but it is probably naive to assume that there is no dependence of the minimum mean free path on the vacancy concentration. In any case, a rough calculation of the saturation resistance is in reasonable agreement with the measurements, and the concept of a minimum mean free path that is related to the lattice constant seems to be verified for the materials.

Electron-lattice-coupling parameters can be calculated from the resistivity data and the Hall coefficients, although optical studies give a more reliable estimate of the plasma frequency. Moreover, superconducting transition temperatures can be estimated from the various parame-

ters, all of which are experimentally determined. The predicted transition temperatures are consistent with the lack of superconductivity in the group-IVB transition-metal carbides. It is interesting that the electron-phonon coupling as measured by the temperature derivative of the resistivity is as large or larger than that of the superconducting group-VB transition-metal carbides.¹ Hence, the group-IVB materials are not superconducting because their carrier densities and plasma frequencies are low. The carrier density increases substantially as the carbon content of the materials decreases, but this increase is offset by a corresponding reduction in electron-phonon coupling that is revealed by the temperature derivative of the resistivity.

ACKNOWLEDGMENTS

This research was sponsored by the Division of Materials Sciences, U.S. Department of Energy, under Contract No. DE-AC05-84OR21400 with Martin Marietta Energy Systems, Inc., and Contract No. DE-FG05-88ER48344 with Oklahoma State University.

*Also at Oklahoma State University, Stillwater, OK 74078.

†Permanent address: Department of Physics, Oklahoma State University, Stillwater, OK 74078.

¹C. Y. Allison, C. B. Finch, M. D. Foegelle, and F. A. Modine, *Solid State Commun.* **68**, 387 (1988).

²L. E. Toth, *Transition Metal Carbides and Nitrides* (Academic, New York, 1971).

³W. S. Williams, *Progress in Solid State Chemistry*, edited by H. Reiss and J. O. McCaldin (Pergamon, New York, 1971), Vol. 6.

⁴W. S. Williams, *Phys. Rev. A* **135**, 505 (1964).

⁵J. Piper, *J. Appl. Phys.* **33**, 2394 (1962).

⁶J. Piper, *Compounds of Interest in Nuclear Reactor Technology*, Inst. Metals Div. Spec. Rep. No. 3, edited by P. Chiotti and W. N. Miner (Edwards, Ann Arbor, Michigan, 1964).

⁷F. W. Clinard and C. P. Kempter, *J. Less-Common Met.* **15**, 59 (1968).

⁸V. S. Neshpor, S. V. Airapetyants, S. S. Ordan'yan, and A. I. Avgustnik, *Inorg. Mater.* **2**, 728 (1966).

⁹O. A. Golikova, A. I. Avgustnik, G. M. Klimashin, and L. V. Kozlovskii, *Fiz. Tverd. Tela (Leningrad)* **7**, 2860 (1965) [*Sov. Phys.—Solid State* **7**, 2317 (1966)].

¹⁰O. A. Golikova, F. L. Feigel'man, A. I. Avgustnik, and G. M. Klimashin, *Fiz. Tekh. Poluprovodn.* **1**, 293 (1967) [*Sov. Phys.—Semicond.* **1**, 236 (1967)].

¹¹I. Vishnevetskaya, A. Gaisanyak, T. Zapadaeva, and V. Petrov, *High Temp.—High Pressures* **13**, 665 (1981).

¹²L. J. van der Pauw, *Philips Res. Rep.* **13**, 1 (1958).

¹³P. R. Bevington, *Data Reduction and Error Analysis for the Physical Sciences* (McGraw-Hill, New York, 1969).

¹⁴H. Bernstein, in Ref. 6.

¹⁵P. Marksteiner, P. Weinberger, A. Neckel, R. Zeller, and P. Dedericks, *Phys. Rev. B* **33**, 6709 (1986).

¹⁶P. Marksteiner, P. Weinberger, A. Neckel, R. Zeller, and P. Dedericks, *Phys. Rev. B* **33**, 812 (1986).

¹⁷B. M. Klein, D. A. Papaconstantopoulos, and L. L. Boyer, *Phys. Rev. B* **22**, 1946 (1980).

¹⁸J. Klima, *J. Phys. C* **12**, 3691 (1979).

¹⁹A. Neckel, P. Rastl, R. Eibler, P. Weinberger, and K. Schwartz, *J. Phys. C* **9**, 579 (1976).

²⁰H. Ihara, M. Hirabayashi, and H. Nakagawa, *Phys. Rev. B* **14**, 1707 (1976).

²¹J. F. Alward, C. Y. Fong, M. El-Batanouny, and F. Wooten, *Phys. Rev. B* **12**, 1105 (1975).

²²V. I. Potoracha, V. A. Tskhai, and P. V. Geld, *Phys. Status Solidi B* **48**, 119 (1971).

²³F. A. Modine, T. Haywood, and C. Y. Allison, *Phys. Rev. B* **32**, 7743 (1985).

²⁴D. A. Papaconstantopoulos (private communication).

²⁵H. Wiesman, M. Gurvitch, H. Lutz, A. Ghosh, B. Schwartz, M. Strongin, P. B. Allen, and J. W. Halley, *Phys. Rev. Lett.* **38**, 782 (1977).

²⁶Z. Fisk and G. W. Webb, *Phys. Rev. Lett.* **36**, 1084 (1976).

²⁷J. H. Mooij, *Phys. Status Solidi A* **17**, 521 (1973).

²⁸P. B. Allen, *Phys. Rev. B* **36**, 2920 (1987).

²⁹P. B. Allen, T. P. Beaulac, F. S. Khan, W. H. Butler, F. J. Pinski, and J. C. Swihart, *Phys. Rev. B* **34**, 4331 (1986).

³⁰W. L. McMillan, *Phys. Rev.* **167**, 331 (1968).

³¹M. Gurvitch, *Phys. Rev. Lett.* **56**, 647 (1986).